ELSEVIER

Journal of Nuclear Materials 241–243 (1997) 1016–1021

journal of nuclear materials

Section 6. Gas in materials

Hydrogen retention properties of low Z and high Z plasma facing materials

Y. Yamauchi [a,*], T. Hino [a,b], K. Koyama [a], Y. Hirohata [a], T. Yamashina [a]

[a] *Department of Nuclear Engineering, Hokkaido University, Kita-13, Nishi-8, Kita-ku, Sapporo 060, Japan*
[b] *National Institute for Fusion Science, Furo-cho, Chikusa-ku, Nagoya 464-01, Japan*

Abstract

Hydrogen retention properties of isotropic graphite, B_4C converted graphite, SiC converted graphite and tungsten were evaluated by using a technique of thermal desorption spectroscopy after the hydrogen ion irradiation (5 keV, H_3^+) in an ECR ion source. The ratios of retained hydrogen at RT were 3/2, 5/6 and 1/10 for B_4C, SiC and tungsten, respectively, when the retained amount of graphite was normalized unity. B_4C or SiC had two peaks due to detrappings of C–H bond, and B–H or Si–H bond in the thermal desorption spectrum. Tungsten had also two peaks in the range below 1000°C. In the annealing temperature dependences of the retained hydrogen, the ratios of retained hydrogen for tungsten, B_4C and SiC more rapidly decreased with the temperature, compared with the case of graphite. In order to reduce the hydrogen retention, the helium ion irradiation (5 keV, He^+) and the subsequent thermal desorption experiment were conducted after the hydrogen ion irradiation. The reductions of the hydrogen amount for tungsten and B_4C were larger than that of isotropic graphite. However, the reduction for SiC was smaller, compared with the case of isotropic graphite.

Keywords: Wall particle retention; Low Z wall material; High Z wall material

1. Introduction

Graphite has been recognized as an excellent plasma facing material (PFM) due to low atomic number and high thermal shock resistance [1,2]. However, the graphite has several disadvantages as PFM, a large hydrogen retention, large sputtering yield [3,4] and so on. If the amount of retained hydrogen in the plasma facing wall becomes larger, the hydrogen more re-emits into the plasma during the discharge, and then the hydrogen recycling shall be enhanced. So, it is necessary to develop a suitable conditioning method and modify the plasma facing wall for the reduction of hydrogen retention. In order to suppress the chemical erosions, the boronization [5–9] or siliconization [10,11] has been employed to coat on the graphite inner walls. In addition, it has been considered to use a high Z material such as tungsten due to low activation and low sputtering yield [12–14]. Hydrogen retention and desorption properties of above materials were investigated for several years [15–22]. However, the hydrogen retention properties for numerous low Z and high Z materials may not have been evaluated in the same apparatus and under the same conditions.

In the present study, we examined the hydrogen retention properties of isotropic graphite, B_4C, SiC and tungsten such as the amount of the retained hydrogen and annealing temperature dependence of hydrogen retention. These properties were obtained by using a technique of thermal desorption spectroscopy, after the hydrogen ion irradiation. In addition, the helium ion irradiation was carried out after the hydrogen ion irradiation to reduce the amount of the retained hydrogen.

2. Experiment

The samples were B_4C converted graphite made by Hitachi Chemical [23], isotropic graphite [24] used as the substrate of the B_4C converted graphite, SiC converted graphite (CFC) made by Toyo Tanso [25] and polycrys-

* Corresponding author. Tel.: +81-11 706 6662; fax: +81-11 709 6413; e-mail: yamauchi@apollo.hune.hokudai.ac.jp.

PII S0022-3115(96)00651-4

talline tungsten made by Nilaco Corp. The sample size was 5 mm × 45 mm. The thickness of tungsten is 0.1 mm, and those of other materials are 0.4 mm. The thickness of B_4C layer and SiC layer are 0.1 and 0.5 mm, respectively. The B_4C and SiC converted graphites were produced by the chemical vapor reactions, $2B_2O_3 + 7C \rightarrow B_4C + 6CO$ and $SiO + 2C \rightarrow SiC + CO$, respectively. The surface concentrations of B and Si are approximately 60% and 40%, respectively [23,25]. The purity of the tungsten is 99.95%.

The hydrogen or helium ion irradiations and followed by the thermal desorption spectroscopy (TDS) were performed in the ECR ion irradiation apparatus with a quadruple mass spectrometer (QMS), shown in Fig. 1. Accelerated hydrogen or helium ions were mass-separated by a sector magnet, and introduced into the irradiation chamber. For the measurement of the retained hydrogen, the sample was irradiated by 5.0 keV H_3^+ ions with a flux of 1×10^{15} $H/cm^2 \cdot s$. The average fluence was taken 5×10^{18} H/cm^2, which was estimated from the sample current. This fluence is sufficient for the amount of retained hydrogen to saturate for isotropic graphite and B_4C converted graphite for whole irradiated area [17,18]. After the irradiation, the sample was heated linearly from RT to 1000°C. The temperature was monitored by a thermocouple. The desorption rate of H_2 was quantitatively analyzed by the data of the QMS [26]. The sample holder was not exposed to the hydrogen ion beam. In order to estimate the background hydrogen, the desorption rate of the sample not irradiated was measured. The background pressure during the TDS measurement was 7×10^{-5} Pa. The amount of the retained hydrogen was calculated by integrating the desorption spectrum. In addition, the activation energy of desorption was estimated from the peak temperatures with the different heating rates (10, 50 and 80°C/min) [27]. Only for tungsten, the activation energy was estimated from the peak temperature with the heating rate of 50°C/min under the assumption that the hydrogen desorption is due to first order (detrapping). For the helium ion impact desorption, the He^+ ion with energy of 5 keV was employed. The range of the helium ion fluence was from 5×10^{17} to 3×10^{18} He/cm^2 with a flux of 1×10^{14} $He/cm^2 \cdot s$. After the helium ion irradiation, the sample was similarly heated from RT to 1000°C, and the desorption spectrum of H_2 was similarly obtained to evaluate the reduction rate of the hydrogen retention.

3. Results and discussion

3.1. Hydrogen retention properties

Thermal desorption spectra of H_2 after hydrogen ion irradiation for isotropic graphite, B_4C converted graphite and SiC converted graphite are shown in Fig. 2(a). The fluence of hydrogen ion was 5×10^{18} H/cm^2. The heating rate was 50°C/min. The spectrum of the graphite had only a single symmetric peak at about 800°C. On the other hand, a new peak appeared in addition to the peak at about 800°C, both for the cases of B_4C and SiC converted graphites. Peak temperatures of additional peaks for B_4C and SiC were about 350 and 600°C, respectively. In our previous experiment, the spectra with two desorption peaks were also observed for the case of Fe or Cr doped graphite [28]. Thermal desorption spectrum of H_2 after hydrogen ion irradiation for tungsten is shown in Fig. 2(b). The fluence of hydrogen ion was 5×10^{18} H/cm2. The heating rate was 50°C/min. It is noted that H_2 desorption rate in Fig. 2(b) is one order of magnitude smaller than that in Fig. 2(a). For tungsten, two desorption peaks appeared in the range below 1000°C, similarly for the cases of B_4C

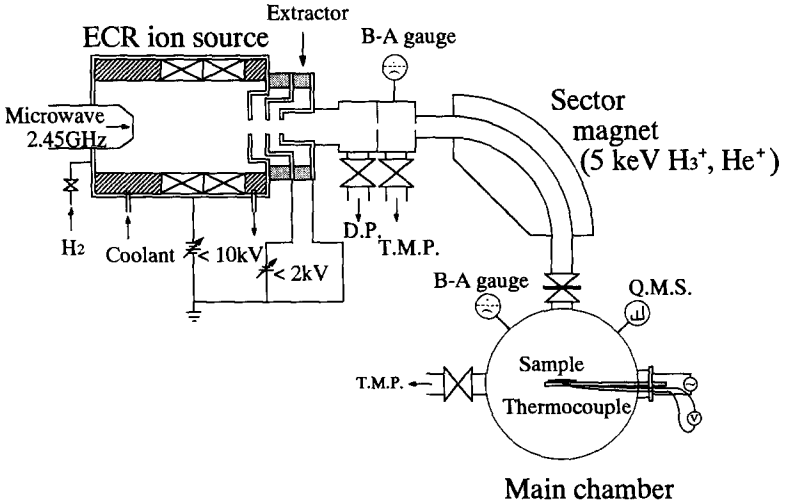

Fig. 1. ECR ion irradiation apparatus.

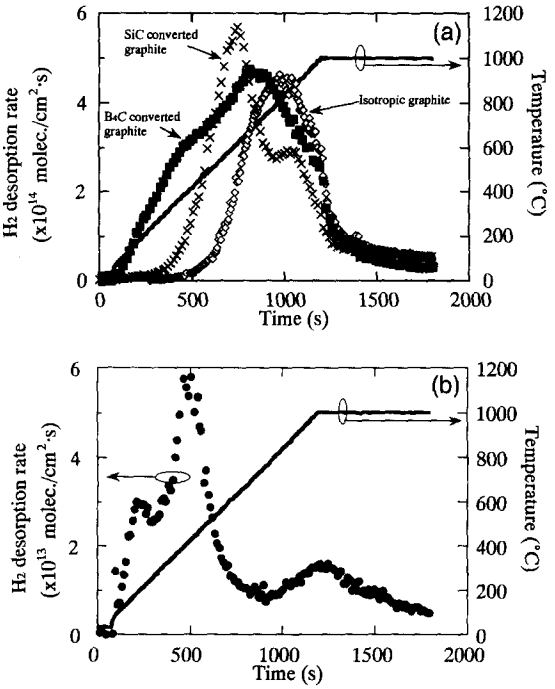

Fig. 2. (a) Thermal desorption spectra of H_2 for isotropic graphite, B_4C converted graphite and SiC converted graphite after hydrogen ion irradiation. (b) Thermal desorption spectrum of H_2 for tungsten.

and SiC converted graphites. The desorption rate increased at around 1000°C, so it is presumed that the spectrum has an additional peak in the range above 1000°C. The peak temperature below 1000°C were 200 and 400°C. It is conceived that the plural peaks are due to the detrappings from the vacancies with different sizes [21].

The activation energies of H_2 desorption from isotropic graphite, B_4C converted graphite, SiC converted graphite and tungsten are shown in Table 1. The activation energies for isotropic graphite, B_4C converted graphite and SiC converted graphite were obtained by changing the heating rate. Only for tungsten, the activation energies was calculated by assuming the first order, e.g. the detrapping. The activation energy of H_2 desorption for isotropic graphite was calculated as about 2.6 eV, which is approximately the same value as that obtained by other authors [15,16]. For the case of SiC, the activation energies of higher temperature peaks are approximately similar to that of isotropic graphite. So, it is regarded that the peaks at lower temperature and higher temperature are due to the detrapping of Si–H and C–H bond, respectively [25]. For the B_4C converted graphite, it is similarly assumed that the lower and higher temperature peaks correspond to the detrappings of B–H and C–H bonds, respectively [23]. For tungsten, the activation energies of H_2 desorption are also similar to the values obtained by other authors [21,22].

After the hydrogen ion irradiation, the major gas species detected by the quadruple mass spectrometer were only H_2 and CH_4. So, the total amount of retained hydrogen was calculated from desorption amounts of H_2 and CH_4. The total amounts of retained hydrogen at RT for above materials were shown in Table 2, with H_2 and CH_4 desorption amounts. The CH_4 desorption amounts of B_4C and SiC converted graphites, i.e. chemical sputtering yields, were approximately 10 times smaller than that of the isotropic graphite. The total amounts of retained hydrogen of the B_4C and SiC converted graphites were roughly comparable with that of the isotropic graphite, e.g., 3/2 and 5/6 of the amount of isotropic graphite, respectively. On the other hand, the amount of hydrogen retained in tungsten was obtained as 6.8×10^{16} H/cm^2, which is 10 times smaller than those of other materials. The hydrogen amounts desorbed at lower temperature were estimated from peak separation. For B_4C and SiC converted graphites, the hydrogen desorbed at lower temperature were 25% and 70% of the total retained amount, respectively. In the same way, the hydrogen amount retained in lower temperature was estimated about 10% of the total amount for the case of tungsten.

From the thermal desorption spectra of H_2 and CH_4 obtained after the irradiation at RT, the fraction of retained hydrogen was obtained as a function of annealing temperature. In the annealIng, the ramp rate was 50°C/min. Fig. 3 shows the annealing temperature dependences of retained hydrogen for isotropic graphite, B_4C, SiC converted graphites and tungsten. In Fig. 3, the hydrogen amount retained at RT is normalized unity. Since the heating rate is not sufficiently low, these data are not in the equilibrium state. However, these data are useful to compare the temperature dependences of the present materials. For the

Table 1
Activation energies of H_2 desorption for isotropic graphite, B_4C converted graphite, SiC converted graphite and tungsten

Sample	Isotropic graphite	B_4C converted graphite		SiC converted graphite		Tungsten	
		low T	high T	low T	high T	low T	high T
Activation energy (eV)	2.6 [a]	1.2 [a]	1.7 [a]	2.2 [a]	2.5 [a]	1.3 [b]	2.0 [b]

[a] Activation energies obtained by changing the heating rate (10, 50, 80°C/min).
[b] Activation energies based on the first order (detrapping).

Table 2
The amounts of total retained hydrogen, H_2 and CH_4 desorptions after hydrogen ion irradiation

	Isotropic graphite	B_4C converted graphite	SiC converted graphite	Tungsten
Desorption amount				
H_2 (molecules/cm^2)	2.5×10^{17}	5.0×10^{17}	2.9×10^{17}	3.4×10^{16}
CH_4 (molecules/cm^2)	4.2×10^{16}	8.1×10^{15}	3.4×10^{15}	~ 0
Total amount of retained hydrogen (atoms/cm^2)	6.7×10^{17}	1.0×10^{18}	5.8×10^{17}	6.8×10^{16}

graphite, the ratio of retained hydrogen began to decrease at the temperature of 500°C. For other materials, the temperature for the ratio to decrease were lower than that of the isotropic graphite. In particular, the decrease began after the heating for the case of tungsten. The temperature for the ratio to become a half for tungsten was ~ 300°C lower, compared with the case of the isotropic graphite (700°C). For the B_4C and SiC converted graphites, those temperatures were also 100°C lower than that of isotropic graphite. The above data show that the baking temperature required is lowest in the case of tungsten.

3.2. Reduction of retained hydrogen by helium ion impact

In order to decrease the hydrogen amount retained in plasma facing wall, the helium discharge cleanings have been often used in fusion devices. Although the energy of helium ion is very high in the present apparatus, we tried to reduce the hydrogen retention by helium ion impact desorption. After the hydrogen ion irradiation, the sample was irradiated by helium ions with an energy of 5.0 keV. After that, the amount of the remained hydrogen was measured by the thermal desorption spectroscopy in the same way.

The H_2 desorption spectra of SiC converted graphite and tungsten after helium ion irradiations are shown in Fig. 4 as examples. The fluence of helium ion was 2.9×10^{18}, 0.5×10^{18} ions/cm^2, for the cases of SiC and tungsten, respectively. For SiC, the total amount of retained hydrogen was about 40% reduced by the helium ion irradiation. In particular, the hydrogen amount in form of Si–H bond largely decreased, about 50%. The hydrogen amount in form of B–H bond was also largely reduced [23]. One possible reason why the reduction of B–H or Si–H bond is larger, is that the binding energy is smaller than that of C–H bond. In the case of tungsten, the low temperature peak almost disappeared by the helium ion impact at this fluence. The total hydrogen amount was 60% reduced, compared with the case before helium ion irradiation.

Fig. 5 shows the helium ion fluence dependences of hydrogen retention for isotropic graphite, B_4C converted graphite, SiC converted graphite and tungsten. In Fig. 5, the retained hydrogen amount before the helium ion irradiation was normalized unfty. The total amount of retained

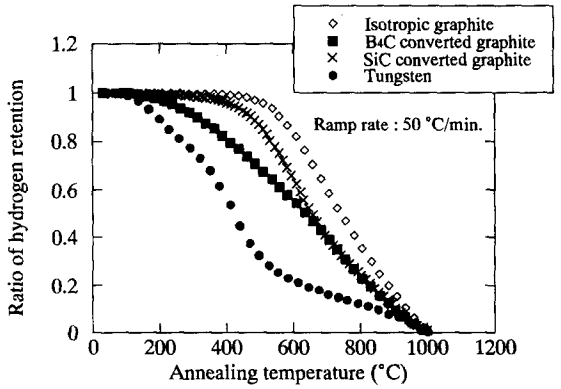

Fig. 3. Annealing temperature dependences of retained hydrogen for isotropic graphite, B_4C converted graphite, SiC converted graphite and tungsten.

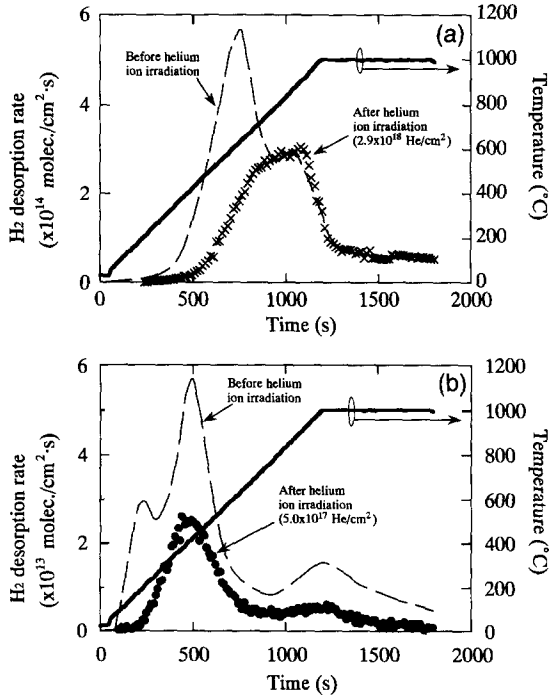

Fig. 4. (a) Thermal desorption spectrum of H_2 for SiC converted graphite after helium ion irradiation. (b) Thermal desorption spectrum of H_2 for tungsten after helium ion irradiation.

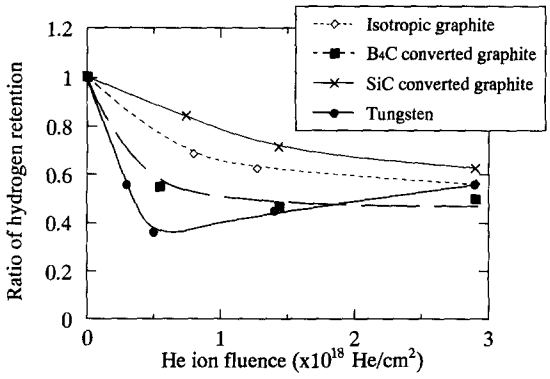

Fig. 5. Helium fluence dependences of retained hydrogen for isotropic graphite, B_4C converted graphite, SiC converted graphite and tungsten.

hydrogen rapidly decreased within the fluence range up to about 1×10^{18} He/cm^2 for all materials. In particular, the hydrogen retention of tungsten had a minimum value at fluence of about 5×10^{17} He/cm^2. It is conceived that the increase of hydrogen retention is due to the retrapping of residual hydrogen on the damaged surface by the helium ion irradiation. On the other hand, the amount of retained hydrogen gradually decreased as helium ion fluence for other materials. Within the present materials, the reduction of the hydrogen amount in SiC converted graphite was smallest.

4. Summary

The hydrogen retention properties and the effects of helium ion impact desorption for isotropic graphite, B_4C converted graphite, SiC converted graphite and tungsten were investigated with a technique of thermal desorption spectroscopy. Two desorption peaks appeared in H_2 desorption spectra for the cases of B_4C, SiC and tungsten. The amount of retained hydrogen at RT in B_4C converted graphite or SiC converted graphite was roughly comparable with that of isotopic graphite. The hydrogen amount retained in tungsten, however, was approximately 10 times smaller than those of other materials. In the annealing temperature dependences of the hydrogen retention, the retained hydrogen of tungsten most rapidly decreased with the temperature. The temperature for the hydrogen amount to become a half was 200–300°C lower than those of the other materials.

The amount of the retained hydrogen was 40–60% reduced due to the helium ion impact desorption for the present materials. The ratio of the reduction was largest in the case of tungsten. It was observed that the hydrogen desorbed at low temperature more largely decreased by the helium ion bombardment, compared with hydrogen desorbed at high temperature.

Acknowledgements

This work was conducted as one of the collaboration study programs of National Institute of Fusion Science. The authors acknowledge the offers of specially prepared samples by Toyo Tanso Ltd. and Hitachi Chemical Ltd.

References

[1] T. Yamashina and T. Hino, Appl. Surf. Sci. 48/49 (1991) 483.
[2] T. Hino and T. Yamashina, Tanso 130 (1987) 118.
[3] E. Vietzke, T. Tanabe, V. Philipps, M. Erdweg and K. Flaskamp, J. Nucl. Mater. 145–147 (1987) 425.
[4] T. Hino, T. Yamashina, S. Fukuda and Y. Takasugi, J. Nucl. Mater. 186 (1991) 54.
[5] M. Saidoh, H. Hiratsuka, T. Arai, Y. Neyatani, M. Shimada and T. Koike, Fusion Eng. Des. 22 (1993) 271.
[6] M. Saidoh, N. Ogiwara, M. Shimada, T. Arai, H. Hiratsuka, T. Koike, M. Shimizu, H. Ninomiya, H. Nakamura, R. Jimbou, J. Yagyu, T. Sugie, A. Sakasai, N. Asakura, M. Yamage, H. Sugai and G.L. Jackson, Jpn. J. Appl. Phys. 32 (1993) 3276.
[7] Y. Hirooka, R. Conn, R. Causey, D. Croessmann, R. Doerner, D. Holland, M. Khandagle, T. Matsuda, G. Smolik, T. Sogabe, J. Whitley and K. Wilson, J. Nucl. Mater. 176–177 (1990) 473.
[8] J. Winter, H.G. Esser, L. Könen, V. Phillips, H. Reimer, J. v. Seggern, J. Schlüter, E. Vietzke, F. Waelbroeck, P. Wienhold, T. Banno, D. Ringer and S. Veprek, J. Nucl. Mater. 162–164 (1989) 713.
[9] J. Winter, J. Nucl. Mater. 176–177 (1990) 14.
[10] G. Hopkins and P. Trester, General Atomics Report, GA-A 17373 (1983).
[11] U. Samm. P. Bogen, G. Esser, J.D. Hey, E. Hintz, A. Huber, L. Könen, Y.T. Lie, Ph. Mertens, V. Phillips, A. Pospieszczyk, D. Rusbüldt, J.v. Seggern, R.P. Schorn, B. Schweer, M. Tokar', B. Unterberg, E. Vietzke, P. Wienhold and J. Winter, J. Nucl. Mater. 220–222 (1995) 25.
[12] Y. Hirooka, M. Bourham, J.N. Brools, G. Chevalier, R.W. Conn, W.H. Eddy, J. Gilligan, M. Khandagle and Y. Ra, J. Nucl. Mater. 196–198 (1992) 149.
[13] J. Roth, J. Nucl. Mater. 176–177 (1990) 132.
[14] T. Noda, Jpn. J. Plasma Fusion Res. 70 (1994) 628.
[15] W. Möller, J. Nucl. Mater. 162–164 (1989) 138.
[16] A. Miyahara and T. Tanabe, J. Nucl. Mater. 155–157 (1988) 49.
[17] B.L. Doyle, W.R. Wampler, D.K. Brice and S.T. Picraux, J. Nucl. Mater. 93–94 (1980) 511.
[18] R. Jimbou, M. Saidoh, N. Ogiwara, T. Ando, K. Morita and Y. Muto, J. Nucl. Mater. 196–198 (1992) 958.
[19] V.Kh. Alimov. R. Schwörer, B.M.U. Scherzer and J. Roth, J. Nucl. Mater. 187 (1992) 191.
[20] V. Fernandez, J. Bardon, E. Gauthier and C. Grisolia, J. Nucl. Mater. 196–198 (1992) 1022.
[21] H. Eleveld and A. van Veen, J. Nucl. Mater. 212–215 (1994) 1421.

[22] A.A. Pisarev, A.V. Varava and S.K. Zhdanov, J. Nucl. Mater. 220–222 (1995) 926.
[23] Y. Yamauchi, Y. Hirohata, T. Hino, T. Yamashina, T. Ando and M. Akiba, J. Nucl. Mater. 220–222 (1995) 851.
[24] M. Yamamoto, T. Ando, H. Takatsu, M. Shimizu, T. Arai, K. Kodama, H. Horiike, K. Teruyama, A. Kiuchi and Y. Goto, Evaluation Tests on First Wall and Divertor Plate Materials for JT-60 Upgrade, JAERI-M 90–119 (1990).
[25] Y. Yamauchi, T. Hino, Y. Hirohata and T. Yamashina, Vacuum 47 (1996) 973.
[26] Y. Nakayama, S. Fukuda and T. Yamashina, J. Vac. Soc. Jpn. 32 (1989) 301.
[27] P.A. Redhead, Vacuum 12 (1962) 203.
[28] S. Fukuda, T. Hino and T. Yamashina, J. Nucl. Mater. 162–164 (1989) 997.